



# Dynamics of flexible peptides under the action of an electrostatic field in the gas phase



Iraklis Litinas, Andreas D. Koutselos \*

National and Kapodistrian University of Athens, Department of Chemistry, Physical Chemistry Laboratory, Panepistimiopolis, 15771 Athens, Greece

## ARTICLE INFO

### Article history:

Received 25 April 2017

Received in revised form 5 July 2017

Accepted 13 July 2017

Available online 14 July 2017

### Keywords:

Flexible macromolecule

Conformation dynamics

Ion Mobility Spectrometry

Nonequilibrium Molecular Dynamics

Simulation

## ABSTRACT

The Ion Mobility Spectrometry data of flexible peptides have been found to depend on the temperature of the buffer gas. It has been observed that the number of the peaks of the arrival time distribution may vary, while the position of the peaks may shift with temperature. Such changes depend on the emerging conformers at the experimental conditions. The motion and the dynamics of the peptide are reproduced here through a Non-equilibrium Molecular Dynamics Simulation procedure that depends on the structure of the bending macromolecule. A specific molecular model of one bending mode is considered that depends on an angular interaction potential. The observed conformations are introduced through the consideration of local minima in the model potential. As the molecular dynamics simulation proceeds, the population of the metastable structures is changing in time due to energy exchange during the ion-atom interactions. The corresponding angle distributions depend on the temperature and the field strength. We find that the observed motion of the peptide conformers can be reproduced accurately with the use of empirical model potentials and further predict the behavior of the ions at strong electric fields. The procedure can produce mean properties, such as the ion velocity and energy, as well as molecular distributions and dynamic properties, such as velocity correlation functions. We expect the method to apply to similar flexible macromolecules that acquire one bending mode.

© 2017 Elsevier B.V. All rights reserved.

## 1. Introduction

The motion of flexible macromolecular ions through gases under the action of weak electrostatic field in Ion Mobility Spectrometry, IMS, presents characteristic features that depend on temperature. The measured arrival time distribution may acquire multiple peaks, due to the appearance of various conformers, or shift abruptly in the time axis as the temperature of the buffer gas varies. The latter continuous modification corresponds to variation of the mean (drift) velocity of the ions, which is associated directly to its cross section in the particular gas, often He. The experimental cross sections contain contributions from different relatively stable conformers, the abundance of which depends on the temperature, as well as from molecular structures that fluctuate between various locally stable forms during the ion flight through the IMS drift tube. Here, again, the relative population around the metastable structures may vary with temperature due to thermal excitation or/and due to temperature induced permanent molecular deformation. Such behavior has been observed in sodiated oligomers [1,2], protonated oligopeptides [3,4], where the changes of the secondary structure are accompanied with intramolecular proton transfer and in oligopeptides that adopt a helix–turn–helix motif [5–8].

Due to the extent of the macromolecules there have not been attempts for all-atom molecular dynamics simulations of the transport and dynamics of the ions but only the determination of possible conformations through a stochastic Monte Carlo annealing procedure. To study the evolution of flexible macromolecules in time, we employ a Non-equilibrium Molecular Dynamics, NEMD, method that we have developed and tested successfully before using a model flexible molecular structure and apply it to a prototype system of the oligopeptide  $\text{AcA}_{14}\text{KG}_3\text{A}_{14}\text{K} + 2\text{H}^+$ , (A = alanine, K = lysine, G = glycine, Ac = acetyl group).

The peptide consists of two rather rigid polyalanine  $\alpha$ -helices connected by three glycine residues, as they have low helix propensity. The lysine residues are both protonated and thus carry the ion charge, with the proton at the C-terminus stabilizing the polyalanine helix by interacting with the helix dipole [9]. Conformational changes have been revealed from the ion–He averaged cross sections obtained from the experimental mobility through the formula [10]

$$K = \frac{3Ze}{16N} \left( \frac{2\pi}{\mu k_b T_{\text{eff}}} \right)^{1/2} \frac{1}{\Omega^{1.1}} \quad (1)$$

The ion mobility  $K$  is given by  $K = v_d/E$ , where  $v_d$  is the drift velocity of the ions parallel to the electric field and  $E$  the field strength.  $Z$ ,  $N$  and  $\mu$  are the charge of the ion, the He gas number density and the reduced

\* Corresponding author.

E-mail address: [akoutsel@chem.uoa.gr](mailto:akoutsel@chem.uoa.gr) (A.D. Koutselos).

ion–He mass respectively. At weak electrostatic fields, the effective temperature  $T_{\text{eff}}$  of the ions is approximated through the Wannier equation [11]

$$(3/2)k_b T_{\text{eff}} \equiv (3/2)k_b T_w = (3/2)k_b T + (1/2)mv_d^2, \quad (2)$$

where  $M$  and  $T$  are the atomic mass and the temperature of the gas respectively. The Wannier temperature,  $T_w$ , at weak electric field and at relatively high temperatures is approximated by  $T$ , as the value of the previous sum is determined mainly by the first term. Furthermore, the kinetic theory collision integral  $\Omega^{1,1}$  is approximated by  $\Omega$ , which represents the ion-atom cross section averaged over all orientations.

Drift tube experiments have shown that at low temperatures, three distinct peaks appear in the drift time spectra, which are attributed to three stable conformations of the ion  $\text{AcA}_{14}\text{KG}_3\text{A}_{14}\text{K} + 2\text{H}^+$ . As the temperature of the buffer gas is raised, two of the three peaks vanish due to thermal destabilization of the relevant conformations and subsequently the remaining peak shifts gradually to times of one of the metastable conformations. Two major inter-converting conformers, one in “extended” and one in “compact” form, appear to explain the shift of the experimental drift time distribution peaks. The two structures are considered to remain intact at low  $T$  but to interchange at high  $T$ , through the opening and closing of the angle between the two  $\alpha$ -helices. A number of candidate relatively stable conformations were determined through an annealing stochastic (Monte Carlo) procedure. Their average ion–He cross sections were calculated through an MD scattering method [7].

Here, we introduce the structural modifications that are attributed to various molecular conformers, through consideration of a bending mode that is characterized by an angular intramolecular potential,  $V(\varphi)$ . The locally stable structures are represented by three minima of the potential that are positioned at three specific bending angles  $\varphi$ . The method has already been employed successfully for the study of the conformation dynamics of the oligopeptide  $\text{RA}_{15}\text{K}$  [12] and the reproduction of the transport and dynamics of small ions in gases under the action of an electrostatic field [13–15]. We calculate the drift velocity and translation, rotation and vibration energies of the ions. In addition we obtain the bending angle distribution and dynamic properties, such as the velocity correlation functions. The ion-atom interaction potential has been determined through a trial and error procedure until the mobility data were reproduced. Further, field dependent mean and dynamic ion properties are predicted at a certain gas temperature.

## 2. Method

Our model consists of two equal hollow cylinders connected by a flexible joint at the edge of their bases. The variation of the angle  $\varphi$  between the axes of the two cylinders, that represents an angular vibration, occurs on the plane defined by the two axes and depends on an interaction potential  $V(\varphi)$ . The presence of a number of local minima in  $V(\varphi)$  reproduces the locally stable conformers of the peptide that make appearance at low temperatures. As the ion moves in the drift tube under the action of the electrostatic field, the excess energy is distributed between the translational, rotational and angular vibrational degrees of freedom. Ions with excited angular vibration may overcome the energy barriers between the minima of the angular potential and change shape. The angular potential is presented in Fig. 1, together with the structure of the modeled peptide.

As restricted to a plane, the angular equations of motion of the flexible peptide are simplified. In total, seven equations of motion have to be integrated for the motion of the peptide to be reproduced. Three degrees for the translational motion, three for the rotational and one for the angular vibration are needed to be followed. The equations for the translational motion in an inertial frame are based on Newton's law with total force exerted on the center of mass (CM) of the modeled peptide. The force includes interactions with the He atoms and the effect of the external electric field. The rotational motion is followed through

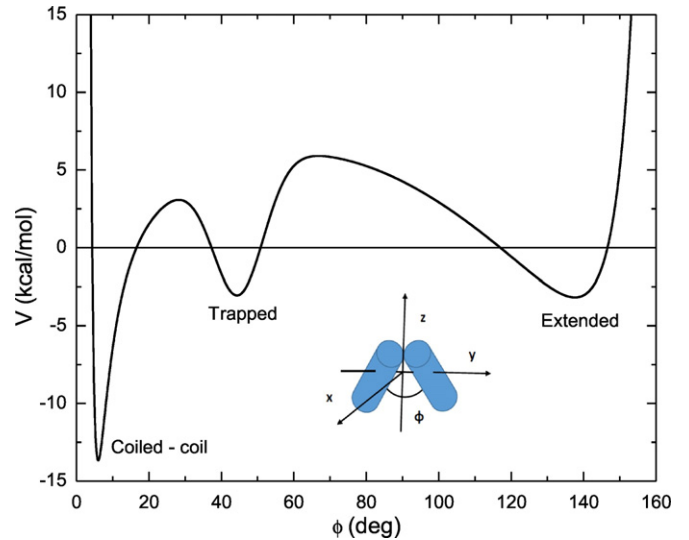


Fig. 1. Angular vibrational potential  $V(\varphi)$  for the folding of a flexible peptide.

Euler's equations of motion, here with time depending moments of inertia  $I$  due to the vibration,

$$\begin{aligned} \tau_x &= I_{xx}\dot{\omega}_x + \dot{I}_{xx}\omega_x + \omega_z \cdot \omega_y \cdot (I_{zz} - I_{yy}), \\ \tau_y &= I_{yy}\dot{\omega}_y + \dot{I}_{yy}\omega_y + \omega_x \cdot \omega_z \cdot (I_{xx} - I_{zz}), \\ \tau_z &= I_{zz}\dot{\omega}_z + \dot{I}_{zz}\omega_z + \omega_y \cdot \omega_x \cdot (I_{yy} - I_{xx}). \end{aligned} \quad (3)$$

All quantities, the torques  $\tau$ , the moment of inertia and the angular velocity  $\omega$  are expressed in the body reference system [12]. Finally, the angular vibration follows an equation obtained through the Lagrangian with kinetic energy

$$T = (1/2)m\mathbf{v}^2 + (1/2)(I_{xx}\omega_x^2 + I_{yy}\omega_y^2 + I_{zz}\omega_z^2) + (1/2)I_\varphi\dot{\varphi}^2 \quad (4)$$

where  $\mathbf{v}$  is the inertial velocity of the CM,  $m$  is the mass of the ion and

$$I_\varphi = (1/4)(2I_{xx}^c + \delta^2 m \cos^2(\alpha + \varphi/2)), \quad (5)$$

with  $I_{xx}^c$  the moment of inertia of a cylinder about its symmetry axis,  $\delta$  the length of the diagonal that connects the cylinder center to the attachment point and  $\alpha$  the angle between the diagonal and the cylinder axis. This quantity resembles a “moment of inertia” for the angular vibration. The equation of motion for  $\varphi$  is

$$\begin{aligned} \ddot{\varphi}I_\varphi - (1/16)\dot{\varphi}^2 m\delta^2(\varphi + 2\alpha) + (1/2)(\omega_z^2 - \omega_y^2)(I_{zz}^c - I_{yy}^c) \sin\varphi \\ - (1/4)m\delta^2(\omega_z^2 - \omega_x^2) \sin(\varphi + 2\alpha) = F_\varphi. \end{aligned} \quad (6)$$

Here,  $F_\varphi$  is the total torque exerted on the cylinders of the peptide due the ion–He interactions, along with the internal forces due to  $V(\varphi)$ . As previously,  $I_i^c$  are the moments of inertia of a cylinder about the “i” body fixed axis. The equations of motion are integrated with the use of the Gear Predictor–Corrector method over a time step of  $10^{-16}$  s [16].

The system under study is out of equilibrium, due to the influence of the external electric field. The potential energy the ions gain from the electric field is continuously dissipated, through the ion–He atoms collisions, and the ions reach a stationary drifting state, though the inert gas, being in excess and in contact to a thermal bath, remains continuously in equilibrium. To maintain the stationary motion of the ions, we employ a method which is based on two parallel molecular dynamics simulation procedures, one for the neutrals that evolve independently from the ions and another for the ions. In the first procedure, we follow the motion of 108 He atoms at ideal conditions of molar volume  $0.02 \text{ m}^3$ .

In the second procedure, the ions move independently of one another and interact with images of the gas particles, which are generated at the start of the ion-atom interaction and erased from the memory of the computer at the end ion-atom encounter. In addition, the ions feel the force exerted by the electric field which here is applied at the center of mass of the peptide. This simplifies the interaction without neglecting important dynamic effects, due to the big mass of the ions relative to the gas atoms. As usually, the interaction starts and ends at a cutoff distance between the ion and the neutral atom,  $R_e = 3.2 \sigma$ , with  $\sigma = 2.556 \text{ \AA}$ , the He distance Lennard-Jones parameter.

In the presence of a weak electric field and for small gradient of ion concentration, as is the case during the most of the flight of the ions in IMS experiments, the ion flux  $\mathbf{J}$  is linear to both field,  $\mathbf{E}$ , and ion density gradient,  $\nabla N$  and is described through the formula

$$\mathbf{J} = N\mathbf{K}\mathbf{E} - D\nabla N. \quad (7)$$

Ion mobility  $K$  and diffusion coefficient  $D$  are scalar transport coefficients and are functions of the (combined) ratio of the field to the density parameter  $E/N$ , which is reported in units of  $T_d$  ( $1 T_d = 10^{-17} \text{ V cm}^2$ ). The ion mobility is calculated through

$$\mathbf{v}_d = \mathbf{K}\mathbf{E}, \quad (8)$$

where  $\mathbf{v}_d$  is the drift velocity in the direction of the field  $\mathbf{E}$ . With the field in the  $z$ -direction, the drift velocity is  $\mathbf{v}_d = \langle v_z \rangle$ . Here, the brackets indicate statistical averages calculated through our molecular dynamics simulation procedure. Further, the mean translational kinetic energies parallel and perpendicular to the field are expressed as effective temperatures through

$$\begin{aligned} E_{\text{tr},x} &= (1/2)k_b T_{\text{tr},x} = (1/2)m \langle (v_x - \langle v_x \rangle)^2 \rangle, \\ E_{\text{tr},y} &= (1/2)k_b T_{\text{tr},y} = (1/2)m \langle (v_y - \langle v_y \rangle)^2 \rangle, \\ E_{\text{tr},z} &= (1/2)k_b T_{\text{tr},z} = (1/2)m \langle (v_z - \langle v_z \rangle)^2 \rangle, \end{aligned} \quad (9)$$

with the field lying parallel to the  $z$  direction at each time step of the simulation, the ensemble averages produce  $\langle v_x \rangle \approx \langle v_y \rangle \approx 0$  and  $\langle v_z \rangle \approx v_d$ , while the cylindrical symmetry of the mean motion imposes that  $\langle (v_x - \langle v_x \rangle)^2 \rangle = \langle (v_y - \langle v_y \rangle)^2 \rangle$ . This is followed within 5% error. At the end of the computation, time averages approach the macroscopic limit and we can set  $T_{\parallel} = T_{\text{tr},z}$  and  $T_{\perp} = \frac{1}{2}(T_{\text{tr},x} + T_{\text{tr},y})$ . The total effective translational temperature can then be calculated through

$$E_{\text{tr}} = (3/2)T_{\text{tr}} = (1/2)T_{\parallel} + T_{\perp}. \quad (10)$$

By analogy, the mean kinetic energies of the ion due to its rotation about the  $x$ ,  $y$ ,  $z$  axis are expressed as effective temperatures through

$$\begin{aligned} E_{\text{rot},x} &= (1/2)k_b T_{\text{rot},x} = (1/2)I_{xx} \langle (\omega_x - \langle \omega_x \rangle)^2 \rangle, \\ E_{\text{rot},y} &= (1/2)k_b T_{\text{rot},y} = (1/2)I_{yy} \langle (\omega_y - \langle \omega_y \rangle)^2 \rangle, \\ E_{\text{rot},z} &= (1/2)k_b T_{\text{rot},z} = (1/2)I_{zz} \langle (\omega_z - \langle \omega_z \rangle)^2 \rangle. \end{aligned} \quad (11)$$

In addition, a total effective rotational temperature is defined through

$$E_{\text{rot}} = (1/3)(T_{\text{rot},x} + T_{\text{rot},y} + T_{\text{rot},z}) \quad (12)$$

In our model, the internal rotational and vibrational degrees of freedom are coupled and therefore an indicative definition for the effective

vibrational temperature,  $T_{\text{vib}}$ , is required. We set

$$E_{\text{vib}} = (3/2)k_b T_{\text{vib}} = \frac{(L_{\varphi} - L_{\varphi_0})^2}{2I_{\varphi}}, \quad (13)$$

with  $L_{\varphi} = I_{\varphi} \dot{\varphi}$  in analogy to the translational effective temperatures.

### 3. Application

We apply our method to study the dynamics and the conformational changes of the twice protonated peptide  $\text{AcA}_{14}\text{KG}_3\text{A}_{14}\text{K} + 2\text{H}^+$  which adopts a helix–turn–helix motif according to IMS study [5–7]. For temperatures less than 250 K three distinct peaks appear in the arrival time distribution, which are attributed to three dominant conformations of the peptide. The first peak, observed at the lowest drift times, is attributed to a compact conformation named coiled-coil. This structure acquires the lowest cross sections. The second peak, appearing at intermediate drift times, is attributed to a trapped conformation whose helices are partly uncoupled having intermediate cross sections. Finally, the third peak with the highest drift times, corresponds to an extended structure of fully uncoupled helices acquiring the highest cross sections.

As the temperature is raised over the 250 K, initially the peaks of the arrival time distribution attributed to the extended and trapped conformations vanish one after the other, supposedly due to their metastable nature, toward the most stable compact form. Above 350 K, however, the remaining peak gradually shifts to arrival times which the open structure ought to acquire. This effect has been interpreted as a conformational change that the flexible peptide undergoes above this temperature. Although many degrees of freedom are involved in conformational changes, it appears that one reaction coordinate is adequate for the description of the molecular transformation, which can be represented effectively by the angle between two stiff parts of the peptide. This peptide has been indeed designed to contain a flexible part of a few glycine residues in between two rather stable polyalanine-helices. To reproduce the experimental results, we employ our model flexible molecular system that resembles in structure to the experimentally studied oligopeptide and calculate the ion transport and dynamic properties at a certain weak field and various gas temperatures, as well as, at one temperature and different field strengths.

#### 3.1. Interaction potentials

We study the ion angular vibration of the flexible peptide by introducing an angular dependent vibrational potential with three minima representing the observed main peptide conformations. The potential, presented in Fig. 1, consists of two main parts

$$V_{n,m}(\varphi) = \sum_{i=1,2} (V_{n,m}^i(\varphi) + V_G^i(\varphi)) \quad (14)$$

The first two terms are cite-cite  $n$ - $m$  type potentials whose general functional form is

$$V_{n,m}^i(\varphi) = \frac{n\varepsilon_i}{n-m} \left[ \frac{m}{n} \left( \frac{\varphi_{m,i} - \alpha_i}{\varphi - \alpha_i} \right)^n - \left( \frac{\varphi_{m,i} - \alpha_i}{\varphi - \alpha_i} \right)^m \right]. \quad (15)$$

Here, we use  $n = 4$  and  $m = 2$ , with parameters  $\alpha_i$  equal to 0 and  $\pi$  for the two  $i$ -terms of the potential. The two minima that correspond to coiled-coil and extended conformations are set at  $\varphi_{m,1} = 6^\circ$  and  $\varphi_{m,2} = 135^\circ$ . The third minimum, which corresponds to the trapped conformation, is represented by two Gaussians of the form

$$V_G^i(\varphi) = \frac{A_i}{\sigma_i \sqrt{2\pi}} \exp\left(-(\varphi - \varphi_{0,i})^2 / 2\sigma_i^2\right) \quad (16)$$

**Table 1**  
Angular potential parameters.

Potential	$\varphi_{m,i}$ or $\varphi_{0,i}$ (deg)	$\varepsilon$ (kcal mol <sup>-1</sup> )	A (kcal mol <sup>-1</sup> )	$\sigma$ (deg)
$V_{4,2}^1(\varphi)$	6	17		
$V_{4,2}^2(\varphi)$	135	6		
$V_6^1(\varphi)$	65		10	50
$V_6^2(\varphi)$	45		-1.5	7

The parameters  $A_i$ ,  $\varphi_{0,i}$  and  $\sigma_i$ , along with the  $\varepsilon_i$  and  $\varphi_{m,i}$  of the  $n$ - $m$  model potentials are presented in Table 1. The latter model potential parameters are in compliance with the theoretical estimation of the potential energy surface of the peptide conformations [17]. The ion-He interaction between the He atom and the cylinder of our model is determined through a 12-6-4 potential

$$V(r) = (\varepsilon_0/2) \left[ (1 + \gamma)(r_m/r)^{12} - 4\gamma(r_m/r)^6 - 3(1 - \gamma)(r_m/r)^4 \right] \quad (17)$$

where  $r_m = 4.92 \text{ \AA}$  and  $\varepsilon_0 = 0.105 \text{ kcal mol}^{-1}$  are the position and the depth of the potential minimum respectively. The first two terms, which are proportional to  $(1/r)^{12}$  and  $(1/r)^6$ , express the short range repulsive and the long range dispersion interaction respectively, while the third term, which is proportional to  $(1/r)^4$ , expresses the long range ion-induced dipole interaction. This term must follow the general expression for the induction interaction

$$V(r) = \frac{e^2 a_d}{2r^4} = \frac{3\varepsilon_0}{2} (1 - \gamma)(r_m/r)^4, \quad (18)$$

where  $a_d$  is the He dipole polarizability [18] from which the  $\gamma$ -parameter becomes  $\gamma = 0.3258$ . This force is exerted perpendicularly to the cylinder axis at distance  $r_0 = 1 \text{ \AA}$  from the axis. The moments of inertia of the hollow cylinders require the consideration of inner and outer radii, set here at  $R_1 = 2.3 \text{ \AA}$  and  $R_2 = 3.0 \text{ \AA}$ , respectively, close to the ones appearing in the literature [19–21]. The length of the cylinders has been estimated from mobility tests to be  $L = 20.8 \text{ \AA}$ . The charge of the peptide is positioned at the cm of the ion. Finally, the He-He interactions are expressed through a Lennard-Jones (12-6) potential [22]

$$V(r) = 4\varepsilon_0 \left[ (\sigma/r)^{12} - (\sigma/r)^6 \right], \quad (19)$$

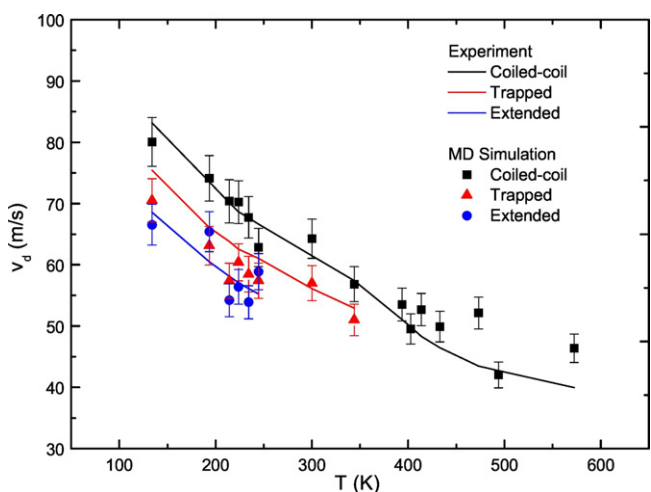


**Fig. 2.** Drift velocities of the three dominant conformers of the peptide ion  $A_{14}KG_3A_{14}K + 2H^+$  as a function of temperature at  $E/N = 10 \text{ Td}$  obtained through the present procedure. The experimental data are estimated from reported cross sections [7] through Eq. (1).

with position of minimum at  $r_m = \sigma\sqrt[6]{2} = 2.869 \text{ \AA}$  and depth  $\varepsilon_0 = 0.0203 \text{ kcal mol}^{-1}$ .

### 3.2. Results

We calculate the mean ion drift velocities of the peptide at 19 temperatures within the experimental range, between 193 K and 572 K. The calculated values, along with those that have been estimated through Eq. (1) using the experimental cross sections [7] data at  $E/N = 10 \text{ Td}$ , are presented in Fig. 2. For all three conformers the drift velocities decrease as the temperature of He is raised, partially because the repulsive part of the potential affects the ion motion. The coiled-coil conformer acquires the highest velocity as expected, because it acquires low collision cross section due to its compact structure. The lowest velocities at low temperatures correspond to the extended conformer due to its unfolded “open” structure that presents large collision cross sections. Finally, the trapped conformer, at intermediate angles, acquires mean velocities in between the previous two. The results are presented with  $\pm 5\%$  error bars as estimated from the numerical. The calculated mean velocities of the trapped and extended structures are compared to the experimental data up to 344 K and 245 K respectively, since the two structures are not detected experimentally at higher temperatures [7]. Between temperatures 300 K and 344 K, the mean velocities are obtained as weighed average of the coiled-coil and the extended structure, while for temperatures higher than 344 K the mean velocity of all three conformers is compared to the experimental data.

The corresponding ion cross sections in He obtained through the Eq. (1) are presented in Fig. 3, as a function of the gas temperature within the experimental range. As the temperature of He is raised the cross sections decrease, partially because the short range repulsive ion-atom interactions dominate and partially due to the increase of contribution of the open peptide structures to the transport. At high temperatures higher percentage of ions are trapped around the extended conformation minimum of the angular potential.

The dependence of the ion mobility versus the field strength at constant gas temperature,  $T = 403 \text{ K}$ , is depicted in Fig. 4. At weak fields the ion mobility increases with the field up to 60 Td, due to the dominance of attractive interactions. At higher fields, the mobility decreases as the repulsive part of the ion-atom potential contributes to the interactions. The mean translation, rotation and vibration energies, presented in Fig. 5, all lie close to one another and to the He temperature, as expected at weak fields. At strong field strengths, however, the translation energy

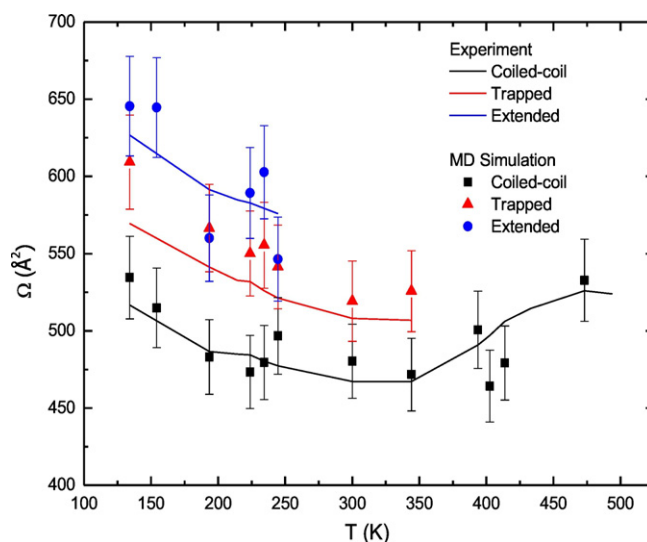


**Fig. 3.** Effective cross sections of the three dominant conformers of the peptide ion presented as in Fig. 2. The experimental data are from reference [7].

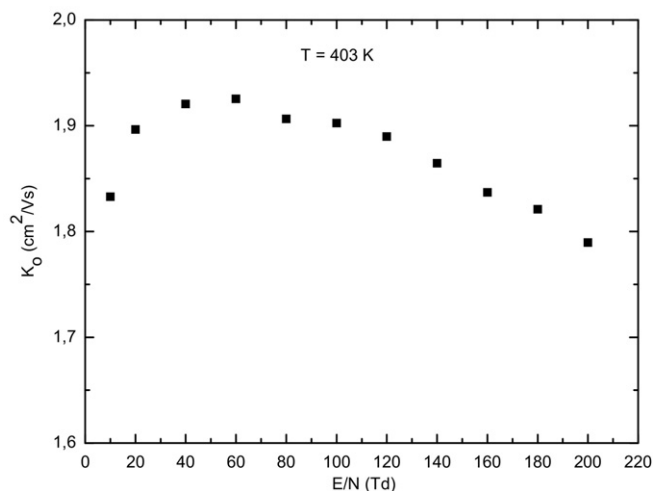


Fig. 4. Standard mobility of the peptide ion  $A_{14}KG_3A_{14}K + 2H^+$  in He as a function of field strength at 403 K.

of the ions is seen to increase above the thermal energy of the gas due to the fact that at strong fields the gas cannot dissipate efficiently all the excess ion translation energy. We mention that the error in these data is quite higher than in the other curves because they are obtained from the subtraction of three orders of magnitude larger quantities, which are the total ion translation energy and the ordered kinetic energy,  $(1/2)mv_d^2$ .

#### 4. Conclusions

The transport and dynamic properties of the oligopeptide  $AcA_{14}KG_3A_{14}K + 2H^+$  in low density He gas under the action of an electrostatic field have been studied through the use of a NEMD simulation method and the introduction of a flexible molecular model for the interactions of the macromolecular ion. The oligopeptide adopts a helix-turn-helix motif where the two  $A_{14}K$  helical sections are linked by a loop of three glycine residues [7]. This structure is represented by two equal size hollow cylinders connected flexibly at the rim, the angle of which depends on an intramolecular potential. Local potential minima at large and small angles have been introduced to represent the extended and compact conformers, as well as one at intermediate angles for all

the possible metastable structures. The variation of the bending angle of the model is followed through the appropriate Lagrange equations of motion. We have used a 12–6–4 model potential for the peptide ion–He interactions and a (12–6) Lennard-Jones potential, for the interaction between the atoms of the inert gas.

The angular potential model is found to be adequate for the description of the motion of the peptide conformers in IMS measurements since it reproduces, within the calculation accuracy, the temperature dependence of the experimental collision cross sections. At low temperature the measured collision cross sections of the conformers are distinct, characteristic to three representative conformations. Around  $T = 350$  K, the slower peptide species are thermally destabilized and transform to the more stable coiled-coil structure, which is the fastest moving through the drift tube. However, as the temperature is raised over the 350 K the cross section of the stable conformer shift to values characteristic to cross section of the extended structure. This shift is reproduced here through the increase of the ion population with kinetic energy above the potential barrier, allowing them to change conformation and eventually to populate the local minimum of the (excited) extended form of the angular potential.

Except from varying the temperature at constant electric field, we have performed MD simulations at constant temperature and various electric field strengths of  $E/N$  at the range 10 Td–200 Td. The dependence of the mobility on the field presents a maximum at 60 Td that corresponds to the dominance of interactions around the ion-atom potential minimum [10]. At this field, the translation energy of the ions starts to deviate from the energies obtained close to equilibrium, at constant field  $E/N = 10$  Td, and varying gas temperature. The internal energy of the peptide ions, however, is not excited and remains equal to the (near) equilibrium values.

The NEMD simulation procedure, using the present flexible peptide model, reproduces the ion mobility experimental results quite accurately. Similar performance is expected to other flexible macromolecules that bend at one point and their folding is described by a single reaction coordinate. We mention that the method can treat temperature dependent interactions that may appear in deforming species at high temperatures.

#### Acknowledgments

The authors acknowledge the computational time granted by the Greek Research & Technology Network (GRNET) in the National HPC–ARIS facility.

#### Funding

This research did not receive grant from funding agencies in the public, commercial, or non-for-profit sectors.

#### References

- [1] J. Gidden, A.T. Jackson, J.H. Scrivens, M.T. Bowers, *Int. J. Mass Spectrom.* 188 (1999) 121.
- [2] J. Gidden, T. Wyttenbach, A.T. Jackson, J.H. Scrivens, M.T. Bowers, *J. Am. Chem. Soc.* 122 (2000) 4692.
- [3] M. Kohtani, T.C. Jones, R. Sudha, M.F. Jarrold, *J. Am. Chem. Soc.* 128 (2006) 7193.
- [4] M. Kohtani, J.E. Schneider, T.C. Jones, M.F. Jarrold, *J. Am. Chem. Soc.* 126 (2004) 16981.
- [5] D. Kaleta, M.F. Jarrold, *J. Am. Chem. Soc.* 125 (2003) 7186.
- [6] M.F. Jarrold, *Phys. Chem. Chem. Phys.* 9 (2007) 1659.
- [7] L.W. Zilch, D. Kaleta, M. Kohtani, R. Krishnan, M.F. Jarrold, *J. Am. Soc. Mass Spectrom.* 18 (2007) 1239.
- [8] S. Consta, J.K. Chung, *J. Phys. Chem. B* 115 (2011) 10447.
- [9] B.S. Kinnear, M.R. Hartings, M.F. Jarrold, *J. Am. Chem. Soc.* 123 (2001) 5660.
- [10] E.A. Mason, E.W. McDaniel, *Transport Properties of Ions in Gases*, Wiley, New York, 1988.
- [11] L.A. Viehland, R.E. Robson, *Int. J. Mass Spectrom. Ion Process.* 90 (1989) 167.
- [12] I. Litinas, A.D. Koutselos, *J. Phys. Chem. A* 119 (2015) 12935.
- [13] G. Balla, A.D. Koutselos, *J. Chem. Phys.* 119 (2003) 11374.
- [14] A.D. Koutselos, *J. Chem. Phys.* 125 (2006) 244304.
- [15] A.D. Koutselos, *J. Chem. Phys.* 134 (2011) 194301.

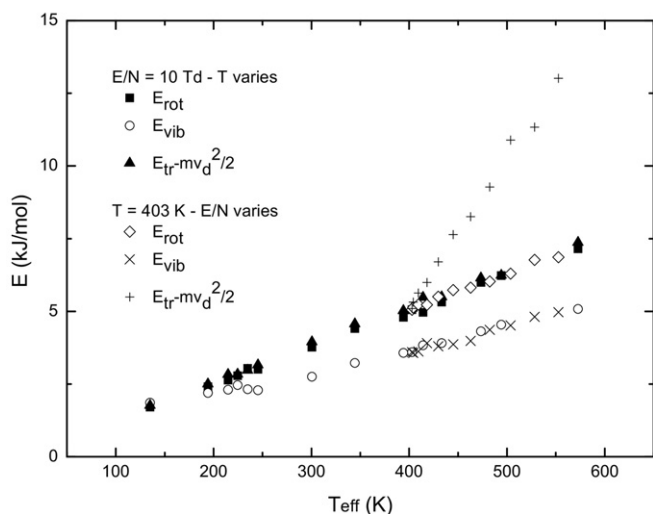


Fig. 5. Mean translation, rotation and vibration energies of the peptide ion  $A_{14}KG_3A_{14}K + 2H^+$  in He. The curves with black triangle and cross are obtained by subtracting the mean energy of the ordered motion,  $mv_d^2/2$ , from the total translation energy,  $E_{tr} = (1/2)m(v_x^2 + v_y^2 + v_z^2)$ .

- [16] M.P. Allen, D.L. Tildesley, *Computer Simulation of Liquids*, Clarendon Press, Oxford, 1987.
- [17] G. Brancolini, A. Venturini, F. Zerbetto, *Theor. Chem. Accounts* 118 (2007) 25.
- [18] A.J. Thakkar, *J. Chem. Phys.* 75 (1981) 4496.
- [19] W. Yu, C.F. Wong, J. Zhang, *J. Phys. Chem.* 100 (1996) 15280.
- [20] R. Raucci, G. Colonna, G. Castello, S. Costantini, *Int. J. Pept. Res. Ther.* 19 (2013) 117.
- [21] F.H.C. Crick, *Acta Cryst* 6 (1953) 689.
- [22] J.O. Hirschfelder, C.F. Curtiss, *Molecular Theory of Gases and Liquids*, John Wiley, New York, 1964 (Appendix I).